Eng. Sci., 2021, **16**, 244–258

Engineered Science
DOI: https://dx.doi.org/10.30919/es8d539

Effect of Camshaft Speed and Packing Thickness on a Multistage Reciprocating Dehumidifier using Analytical Approach

Sampath Suranjan Salins,[1] S.V. Kota Reddy[2] and Shiva Kumar[3,*]

Abstract

Humidity in the living room needs be regulated to maintain thermal comfort. Liquid desiccant dehumidification proved to be an effective and environmentally friendly way of dehumidifying air compared to conventional air conditioning units. The present paper focuses on designing and fabricating the dehumidifier unit where the packing is in dynamic motion. Four Celdek 7090 packings are positioned at different positions reciprocated using cam follower mechanism. When the air circulates through the duct, dehumidification performance parameters such as moisture effectiveness, moisture removal rate and mass transfer coefficient are determined. A mathematical model is constructed, and performance prediction is carried out for different camshaft speed and the packing thickness. The prediction results are compared with the experimental results. Desiccant concentration at the outlet is determined using both approaches. Results indicated that the system gave moisture effectiveness, moisture removal rate and mass transfer coefficient equal to 0.77, 2.28 g/s, 14.89 kg/m^2-s. Performance is improved when the cam shaft is increased from 6 to 10 rpm and there afterwards performance is deteriorated. Maximum performance was obtained for 20 mm thick pad.

Keywords: Dehumidification; Desiccant concentration; Mathematical model; Packing thickness; Reciprocating packing.
Received: 28 August 2021; Accepted: 3 October 2021.
Article type: Research article.

1. Introduction

Control of the humidity in a defined space and maintaining thermal comfort is essential to increase human efficiency and health. Temperature and humidity mainly influence the life of the products in the fields such as food processing, manufacturing, storage *etc*.[1] Conventional mechanical refrigeration system decreased the temperature below dew point temperature and dehumidifies the air and reheated to the required temperature. The evaporator in mechanical refrigeration operates at a very low temperature, leading to lower coefficient of performance (COP), higher energy requirements, and polluting the environment.[2,3] To utilize an energy efficient system to minimize the moisture, desiccant dehumidifiers are used. There are mainly two types, solid and liquid desiccant dehumidifiers. In solid desiccant dehumidifiers, desiccants are fed inside the wheel, or a mesh and the air is circulated through it. In this system, dehumidification occurs by adsorption. In liquid desiccant dehumidifiers, the air and desiccant meet in the standard packing and mass transfer takes place by absorption.[4] Liquid desiccants are chemical substances that absorb moisture by removing the latent heat and converting it to sensible heat.[5] The concentration of the desiccant reduces the vapor pressure of the desiccant and since the air vapor pressure is higher, moisture transfer occurs from higher to lower concentrations.[6] Similarly, in the regeneration process, when the energy is added to the desiccant, the hot air vapor pressure inside the regenerator is lower than that of hot desiccant, leading to mass transfer from desiccant to the air, which escapes into the atmosphere. Regeneration can be carried out using electricity, waste heat, natural gas, or solar energy.[7] Some of the critical factors that influence the performance of liquid desiccant dehumidifier system (LDDS) are desiccant concentration,

[1] *Department of Mechanical Engineering. School of Engineering and Information Technology, Manipal Academy of Higher Education, Dubai, 345050, United Arab Emirates.*
[2] *Department of Mechanical Engineering, VIT-AP University, Vijayawada, 522 237, Andhra Pradesh, India.*
[3] *Department of Mechanical and Manufacturing Engineering. Manipal Institute of Technology, Manipal Academy of Higher Education, Manipal, 576104, India.*
**E-mail:* Shiva.kumar@manipal.edu (S. Kumar)

packing material, type of flow, thickness of packing, and packing position.[8] Lithium Bromide and Lithium Chloride are the desiccants that are used abundantly in LDDS. But they have drawbacks such as high corrosiveness and chemical instability. Calcium Chloride is another desiccant that gives good dehumidification and less corrosiveness. Celdek 7090 and Celdek 5090 are commercially available packing used in most LDDS because of consistent performance and high wettability.[9,10] The thickness of the packing is another parameter significantly influencing the dehumidification. Counter flow is very effective among the counter and cross-flow dehumidification types, as it gives maximum mass and heat transfer.

As many variables influence the dehumidification process, conducting experiments by varying all the conditions is a tedious task. Alternatively, system performance can be analyzed by constructing an analytical or numerical technology-based model and simulating it for various input parameters to predict the output responses for different input conditions. Soft computing-based techniques such as Artificial Neural Networks (ANN), fuzzy logic-based optimization techniques are also widely used for output prediction.

Bouzeffour *et al*.[11] used ANN to compare and predict the results for counter flow dehumidifier using $CaCl_2$ as the desiccant. Deviation of 4.90% for MRR and 3.85% for effectiveness between the ANN and experimental results. Oyieke and Inambao[12] adopted the ANN technique, which used cellulose packing and lithium bromide (LiBr) desiccant. MRR and moisture efficiency for the experimental and theoretical results fluctuated by 0.2 g/s and 1.8%. Also, it was found that there was a drop in the MRR and moisture effectiveness with the rise in the inlet air temperature. Overall, the system gave a MRR and effectiveness value of 1.6 g/s and 70% respectively. Zendehboudi *et al*. [13] worked on a cross flow dehumidifier unit, where in experimental results were compared where soft computing techniques such as least square support vector machine (LSSVM), Adaptive Neuro Fuzzy Inference System (ANFIS) and ANN techniques. All three models predicted the results with a deviation of less than 3% compared with the experimental results. Dehumidification effectiveness and mass transfer coefficient were found to be 78% and 6.57 kg/m^2-s. Seenivasan *et al*.[14] used Taguchi method to validate the results of a dehumidifier. The influence of desiccant temperature, concentration, flow rate and relative humidity on dehumidification were studied. Results concluded that, there was a drop in the moisture effectiveness, solution temperature and desiccant concentration with the increase in the air velocity. Yohana *et al*.[15] conducted a computational fluid dynamics analysis where the effect of desiccant concentration, the flow rate of desiccant and air on the dehumidification performance were studied. Lithium Chloride desiccant concentration was maintained at 32%. Simulation results showed that the system gave maximum specific humidity drop with a higher concentration of the liquid desiccant, low air flow rate and high solution flow rate. Dehumidification efficiency of 67% and specific humidity change equal to 8.8 g/kg were obtained. Shen *et al*.[16] carried out computational fluid dynamics method where polycarbonate panels, LiBr, LiCl and $CaCl_2$ were used. Experiments were conducted by varying inlet temperatures and time period. Celdek 7090 was used as packing. A maximum pressure drop of 74 Pa was noticed and system gave a COP of 0.3 to 0.35. An absorber efficiency of 70% was obtained. Tao *et al*.[17] used CFD analysis to analyze the cross flow dehumidifier where the input parameters such as air velocity, air humidity, solution temperature and temperature were used. Celdek packing was used as packing and lithium chloride as the desiccant. Experimental and theoretical results were deviated by 7%. Sreelal *et al*.[18] analyzed the two-phase flow using CFD for the counter flow dehumidifier where the results were compared with the experimental data. Results indicated that exit temperature of the desiccant increased with the air velocity.

Static or stationary packing is used in most cases that faced the issue of salt accumulation over the period.[10] In addition, since the desiccant is continuously sprayed onto the packing, lot of spillage and wastage of the desiccant occurs. Replacement of this extra desiccant becomes very costly in case of good desiccants such as ionic based types. Hence to minimize wastage and to have a very effective system, dynamic packing may be one of the alternatives. It can solve this issue by rotating, oscillating, or reciprocating pads, which will also aid dehumidification. Even though some researchers have used different principles to have a dynamic motion to the pads, not much improvement was observed in the dehumidification performance.

Bassuoni[19] constructed a mathematical model for the counter flow dehumidifier unit where two static pads were used. $CaCl_2$ was used as the desiccant. Experiments and theoretical analysis were carried out by varying air flow rate, inlet specific humidity and desiccant temperature. An increase in desiccant concentration increased the dehumidification performance and the system gave MRR and moisture effectiveness equal to 0.16 g/s & 0.58 respectively. Naik *et al*.[20] worked on a two-stage rotary dehumidifier where the Inlet temperature and humidity values were varied. Experimental results showed that the condensation rate increase with the air velocity and drop in the temperature. A condensation rate of 24 g/s and moisture effectiveness of 64% were obtained. Chengqin *et al*.[21] used LiCl desiccant in a counter flow dehumidifier. The mathematical model and experimentation results reveal that temperature and specific humidity dropped with the increase in the number of heat transfer units (NTU). Outlet Humidity ratio and temperature were found to be 0.035 kg/kg and 33 °C. Babakhani *et al*.[22] worked on a two stage, static packing which integrated dehumidification and regeneration units. Air and liquid flow rate, air temperature and humidity, desiccant temperature were taken as the input variables. System gave Moisture effectiveness and condensation rate equal to 0.8 and 0.6 g/s.

Kumar and Asati[23] used two static packings where the LiCl desiccant and air interacted in cross flow direction. Theoretical results showed that with the rise in the air flow rate, there was an increase in the condensation rate and drop in the dehumidification efficiency. System gave MRR and dehumidification effectiveness equal to 1.2 g/s and 0.70. Englart and Rajski[24] worked on a cross flow hollow membrane module and LiCl is used as a desiccant. Lithium Chloride temperature was set between 14 to 26 ℃ and air flow rate varied from 105 to 110 kg/s. Moisture effectiveness of 0.45 was obtained and experimental and theoretical results gave a deviation of 5%. Salins *et al*.[26] experimented on Four-stage packing that moves in a linear direction powered by the motor. Celdek packing 5090 and $CaCl_2$ liquid desiccant were used. Inlet air flow rate of 3.1 to 8.2 m/s, cam shaft speed of 6 to 21 rpm, inlet RH of 74 to 90% and inlet temperature of 30 to 42 ℃ were varied. System gave MRR of 4.8 g/s and moisture effectiveness of 0.73. Xiong *et al*.[27] worked on a multistage dehumidification experimentation, where the inlet air temperature was varied from 28.2 to 29.5 ℃, desiccant temperature maintained at 27 ℃ and inlet humidity varied from 16.3 to 17.2 g/kg. It was found that COP and exergy effectiveness were 0.70 and 0.26 respectively. Chen *et al*.[28] used two stage packing mechanism where LiCl is used as a desiccant. Ambient temperature was maintained between 25.3 to 27.7 ℃, specific humidity varied from 14 to 18.3 g/kg and solution temperature from 15.5 to 19.25 ℃. The system gave a dehumidification effectiveness of 0.66. Alan *et al*.[29] used LiCl desiccant in the multistage dehumidifier where packing thickness was varied from 0.1 to 1.5 m and air velocity from 0.75 to 3 m/s. The system gave a moisture removal rate of 0.025 kg/kg. De Oliveira *et. al*[30] worked on humidification dehumidification and desalination unit where Celdek 7090 packing was used media and LiCl as desiccant. Inlet temperature was varied from 23 to 35 ℃. They observed a distillate mass flow rate of 1.4 kg/hr at the exit.

Even though many studies have been reported on the single static stage dehumidification, limited study is available in the multistage dehumidification, packing in dynamic motion or more specifically, reciprocating type. As the performance depends on the number of parameters related to the pad motion, air and desiccant characteristics and flow conditions, a theoretical model to predict the output performance of a dynamic reciprocating multistage dehumidifier is not seen in any of the literature. The past literature review shows that soft computing techniques can be used for the output prediction. They have certain limitations such as a huge cluster of data requirements for training, the necessity of high-capacity computer requirements, increased training error, any outlier if at all, leads to inaccurate results. Moreover, the accuracy of test results relies on the algorithm structure and its training. If the limited data set is available may lead to inadequate training and hence inaccurate results. Hence, it is summarized that prediction performance depends largely on the quality and quantity of data set, computational facility, and algorithm architecture.

To overcome the above drawbacks corresponding to dehumidification performance and prediction, a multistage dynamic experimental test rig is constructed where the packing is in reciprocating action. A theoretical model is built using an analytical approach considering all the parameters influencing the dehumidification process. The prediction results are compared with the experimental values for similar operating conditions and the efficacy of the generated analytical model is evaluated.

2. Mathematical model to predict outlet desiccant concentration, temperature, and specific humidity

A packing shown in the Fig. 1 has the wettability or surface density β. L, H and D be the length, height, and depth of the packing. V_p be the packing volume, A_s be the total wetted area of the packing exposed to air and the desiccant. Let L_c be the characteristic length which is a ratio of the surface area to the volume of the packing.

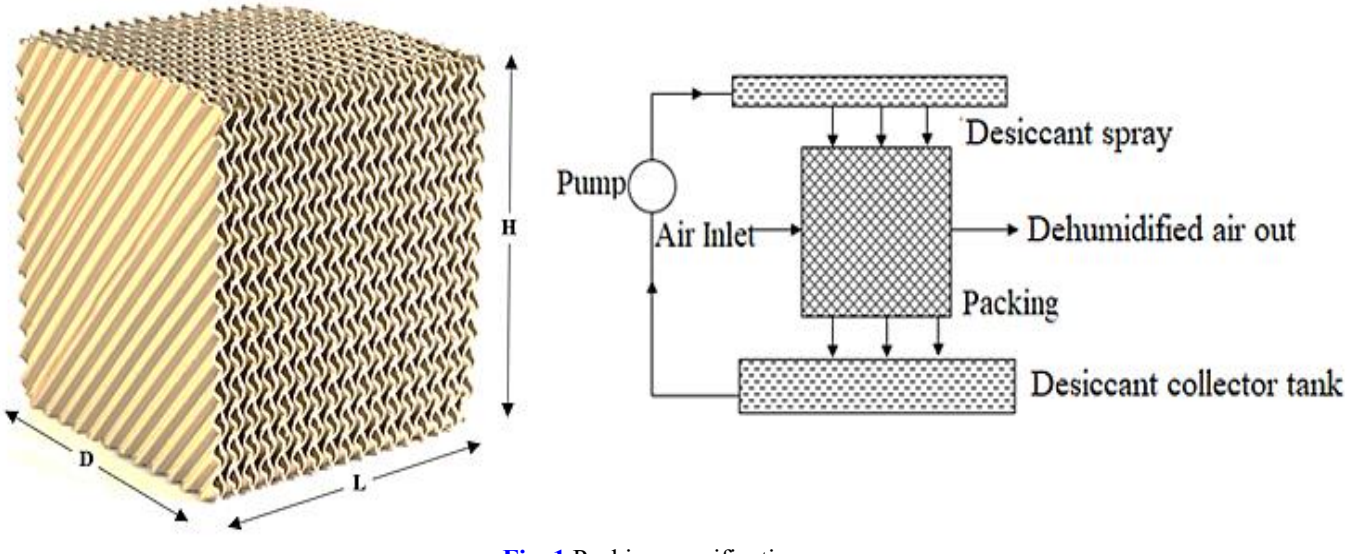

Fig. 1 Packing specifications.

Volume of the pad is given by

$$V_p = L * H * D \quad (1)$$

Wettability and the packing surface area are related using Equation (2) and the characteristic length is the inverse of the wettability given by Equation (3).

$$V_p * \beta = A_s \quad (2)$$

$$L_c = \frac{V_p}{A_s} = \frac{1}{\beta} \quad (3)$$

Considering V as the air velocity, C_P the specific heat, k the thermal conductivity, ν the kinematic viscosity and μ the dynamic viscosity,

Reynolds number Re, Prandtl number and Nusselt number Nu are determined using Equations (4), (5) and (6).

The calculated values are substituted in (7) which yields heat transfer coefficient.

$$R_e = \frac{V * L_C}{\nu} \quad (4)$$

$$P_r = \frac{\mu * C_p}{k} \quad (5)$$

For a corrugated Celdek packing, Nu is expressed by the Equation (6)[25]

$$N_u = 0.1 * \left(\frac{L_c}{L}\right)^{0.12} {R_e}^{0.8} {P_r}^{0.33} \quad (6)$$

$$N_u = \frac{hL_c}{k} \quad (7)$$

Fig. 2 shows the details of the various parameters influencing dehumidification. C_{s1} and T_{s1} are the initial concentration and temperature, whereas C_{s2} and T_{s2} are the desiccant's final concentration and temperature. $\dot{m}_a$ is the mass flow rate of the air, $\dot{m}_{s1}$ and $\dot{m}_{s2}$ be the mass flow rate of the solution at the inlet and outlet. T_1 and T_2 be the air temperature, W_1 and W_2 be the specific humidity at the inlet and outlet. Enthalpy changes when the air moves from inlet to outlet, and ha_1 and ha_2 are the specific enthalpy at the inlet and exit.

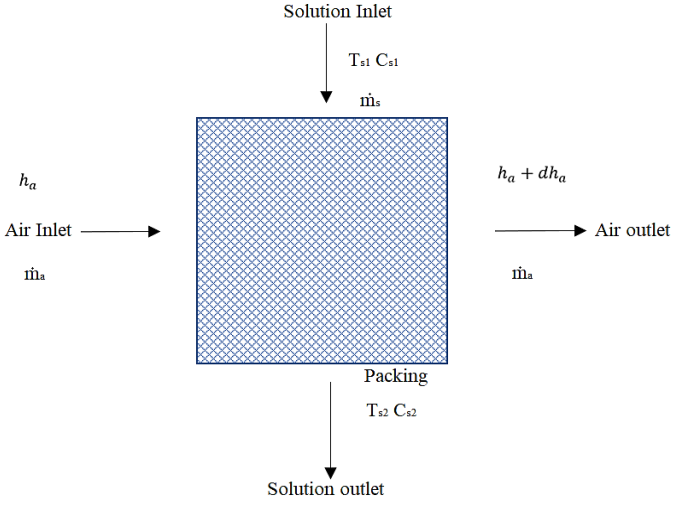

Fig. 2 Parameters of dehumidification.

The assumptions were made to solve the complexity of the fundamental governing equations.

1. De humidifier unit is adiabatic 2. Flow across the pads is steady 3. Airflow rate remains the same at all points 4. Properties of ambient conditions and desiccant remain the same 5. Desiccant solution properties at the interface area are determined by taking the average of the properties across the dehumidifier.

2.1 Outlet concentration

The vapor pressure of the desiccant is lower than the vapor pressure of air that leads to dehumidification. During dehumidification, water that is condensed increases the mass of the desiccant leaving the packing. The condensation flow rate is given in Equation (8)

$$\dot{m}_{condensation} = \dot{m}_a(W_1 - W_2) \quad (8)$$

The mass flow rate of the desiccant is constant when the absorption process takes place. Hence

$$\dot{m}_{s1}C_{s1} = \dot{m}_{s2}C_{s2} \quad (9)$$

Solution mass at outlet = inlet solution mass + condensed moisture

$$\dot{m}_{s2} = \dot{m}_{s1} + \dot{m}_a(W_1 - W_2) \quad (10)$$

Substitute (10) in (9)

$$\dot{m}_{s1}C_{s1} = ((\dot{m}_{s1} + \dot{m}_a)(W_1 - W_2)C_{s2} \quad (11)$$

$$C_{s2} = \frac{\dot{m}_{s1}C_{s1}}{(\dot{m}_{s1} + \dot{m}_a)(W_1 - W_2)} \quad (12)$$

Equation (12) gives the concentration of the desiccant at the outlet undergoing dehumidification.[19]

2.2 Exit Specific humidity in a multistage dynamic packing

Packings are dipped inside the desiccant tank and hence get soaked. When the air passes through the duct, it interacts with the soaked packings and hence dehumidified. Fig. 3 shows the schematic representation of the multistage dehumidification. It shows the position of four reciprocating pads at an instant inside the duct. Let T, W and V represent the temperature, specific humidity, and velocity of the air at various stages in the duct. W_e is the equilibrium-specific humidity.

T_1, T_2, T_3 and T_4: Temperatures at the inlet, exit of the 1st, 2nd, 3rd and 4th packing respectively.

W_1, W_2, W_3, W4: Specific humidities at the inlet, exit of the 1st, 2nd, 3rd and 4th packing respectively.

V_1, V_2, V_3, V_4: Air velocities at the inlet, exit of the 1st, 2nd, 3rd and 4th packing respectively.

Condensation rate = total mass transfer during dehumidification. Equation (13) gives the mass transfer rate conversion.[32]

$$\dot{m}_a dW = K\,\beta\,(W - W_e)L\,dS\,D$$

$$\frac{dW}{(W_e - W)} = -\frac{K\beta\,LD}{\dot{m}_a}\,dS \quad (13)$$

Considering a differential distance dS in linear direction due to the rotation of the camshaft, expressing dS in terms of speed of rotation of the camshaft and the differential pad height dH is shown in Equation (14)

$$dS = dH * 2N \quad (14)$$

Substitute (14) in (13)

Condensation rate = total mass transfer during the dehumidification,

$$\dot{m}_a dW = K\,\beta\,(W - W_e)L\,dS\,D$$

$$\frac{dW}{(W_e - W)} = -\frac{K\beta\,LD}{\dot{m}_a}\,dS \quad (15)$$

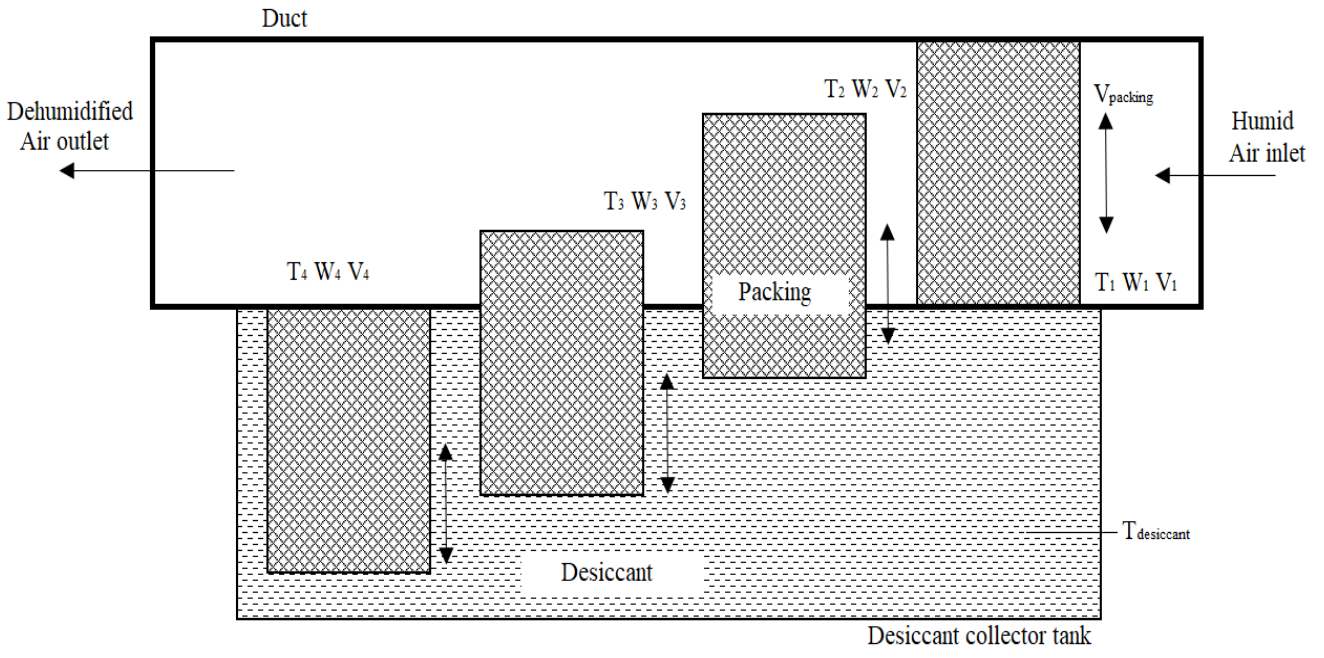

Fig. 3 Multi staged reciprocating dehumidification.

$$\frac{dW}{(W_e - W)} = -\frac{2N\,K\beta\,LD}{\dot{m}_a}\,dH \tag{16}$$

Specific humidity varies from W_1 to W_2, and height varies from 0 to H.

$$\int_{W_1}^{W_2} \frac{dW}{(W_e - W)} = \int_0^H -\frac{2NK\beta\,LD}{\dot{m}_a}\,dH$$

$$\frac{ln(W_e - W_2)}{ln(W_e - W_1)} = -\frac{2NK\beta\,LHD}{\dot{m}_a}$$

$$\frac{(W_2 - W_e)}{(W_1 - W_e)} = e^{-\frac{2NK\beta\,LHD}{\dot{m}_a}} \tag{17}$$

Subtract -1 on LHS and RHS,

$$\frac{(W_2 - W_e)}{(W_e - W_1)} - 1 = e^{-\frac{2NK\beta\,LHD}{\dot{m}_a}} - 1$$

$$\frac{(W_2 - W_e)}{(W_1 - W_e)} - 1 = e^{-\frac{2NK\beta\,LHD}{\dot{m}_a}} - 1$$

$$\frac{(W_2 - W_1)}{(W_1 - W_e)} = e^{-\frac{2NK\beta\,LHD}{\dot{m}_a}} - 1 \tag{18}$$

Multiply -1 on both sides,

$$(W_1 - W_2) = (W_1 - W_e)(e^{-\frac{2NK\beta\,LHD}{\dot{m}_a}} - 1)$$

$$(W_2 - W_1) = (W_e - W_1)(e^{-\frac{2NK\beta\,LHD}{\dot{m}_a}} - 1)$$

$$W_2 = W_1 + ((W_e - W_1)(1 - e^{-\frac{2NK\beta\,LHD}{\dot{m}_a}})) \tag{19}$$

Lewis number is defined as the ratio of heat transfer coefficient to the mass transfer coefficient and specific heat product. Assuming Lewis number Le equal to 1.

$$\frac{h}{KC_p} = L_e \tag{20}$$

Substitute (20) in (19),

$$W_2 = W_1 - ((W_1 - W_e)(1 - e^{-\frac{2Nh\beta\,LHD}{C_p\dot{m}_a}})) \tag{21}$$

Equation (21) gives the specific humidity at the outlet of the packing.

2.3 Outlet temperature:

When the air interacts with the desiccant, specific humidity of airdrops and subsequently a rise in the air temperature occurs due to the heat of condensation. Under adiabatic conditions, Enthalpy of air at the inlet = Enthalpy of air at the outlet, here, h_a is the enthalpy; T_a is the temperature and C_{pa} is the specific humidity of the air. LHV is the latent heat of vaporization.

$$h_a = C_{pa}T_a + W(C_{pv}T_a + LHV) \tag{22}$$

$$\text{Where } C_{pa} = C_{pa} + WC_{pv} \tag{23}$$

Substitute (23) in (22),

$$h_a = (C_{pa} + WC_{pv})T_a + W(C_{pv}T_a + LHV) \tag{24}$$

Differentiate Equation (16),

$$dh_a = (C_{pa} + WC_{pv})dT_a + dW(C_{pv}T_a + LHV) \tag{25}$$

Enthalpy at the inlet is h_a and $h_a + dh_a$ is the enthalpy at the exit. Enthalpy at the inlet and exit is assumed to be same.

$$h_a = h_a + dh_a \tag{26}$$

$$dh_a = 0$$

$$(C_{pa} + WC_{pv})dT_a + dW(C_{pv}T_a + LHV) = 0$$

$$dW(C_{pv}T_a + LHV) = -(C_{pa} + WC_{pv})dT_a \tag{27}$$

Multiply $\dot{m}_a$ in the Equation (27),

$$\dot{m}_a dW(C_{pv}T_a + LHV) = -\dot{m}_a(C_{pa} + WC_{pv})dT_a$$

$$\dot{m}_a dWC_{pv} = -\dot{m}_a(C_{pa} + WC_{pv})dT_a \tag{28}$$

Condensation rate x specific he $= -\dot{m}_a(C_{pa} + WC_{pv})dT_a$.

Heat transfer by convection is responsible for the condensation of the moisture.

$$Heat\ transfer\ by\ convection = -\dot{m}_a(C_{pa} + WC_{pv})dT_a \tag{29}$$

$$Heat\ transfer\ by\ convection = h\,A\,\Delta T \tag{30}$$

Area is given in the form of wettability,

$$A = \beta\,LH\,dD \tag{31}$$

Equations (30) and (29) and Substitute (24) in it,

$$h\beta\ L\ dS\ D(T_s - T_a) = -\dot{m}_a(C_{pa} + WC_{pv})dT_a$$
$$h\beta\ L\ dH\ 2N\ D(T_s - T_a) = -\dot{m}_a(C_{pa} + WC_{pv})dT_a$$
$$\frac{2N\ h\beta\ L\ dH\ D}{\dot{m}_a(C_{pa}+WC_{pv})} = -\frac{dT_a}{(T_s - T_a)} \quad (32)$$

Integrate Equation (32) with respect to the limits 0 to D and T_1 to T_2. Solve the equation to obtain T_2.

$$\int_0^H -\frac{2Nh\beta\ LD\ dH}{\dot{m}_a(C_{pa} + WC_{pv})} = \int_{T_1}^{T_2} \frac{dT_a}{(T_a - T_s)}$$
$$-\frac{2Nh\beta\ LHD}{\dot{m}_a(C_{pa} + WC_{pv})} = \frac{ln(T_2 - T_s)}{ln(T_1 - T_s)}$$
$$-\frac{2Nh\beta\ LH\ D}{\dot{m}_a(C_{pa} + WC_{pv})} = \frac{ln(T_2 - T_s)}{ln(T_1 - T_s)}$$
$$-\frac{2Nh\beta\ LH\ D}{\dot{m}_a(C_{pa} + WC_{pv})} = \frac{ln(T_2 - T_s)}{ln(T_1 - T_s)}$$
$$\frac{(T_2 - T_s)}{(T_1 - T_s)} = e^{-\frac{2Nh\beta\ LH\ D}{\dot{m}_a(C_{pa}+WC_{pv})}}$$
$$\frac{(T_2 - T_s)}{(T_1 - T_s)} - 1 = (e^{-\frac{2Nh\beta\ LH\ D}{\dot{m}_a(C_{pa}+WC_{pv})}} - 1)$$
$$\frac{(T_2 - T_1)}{(T_1 - T_s)} = (e^{-\frac{2Nh\beta\ LH\ D}{\dot{m}_a(C_{pa}+WC_{pv})}} - 1)$$

Multiply -1 on the LHS and RHS,

$$\frac{(T_2 - T_1)}{(T_s - T_1)} = (1 - e^{-\frac{2Nh\beta\ LH\ D}{\dot{m}_a(C_{pa}+WC_{pv})}})$$
$$(T_2 - T_1) = (T_s - T_1)\ (1 - e^{-\frac{2Nh\beta\ LH\ D}{\dot{m}_a(C_{pa}+WC_{pv})}})$$
$$(T_2 - T_1) = (T_s - T_1)\ (1 - e^{-\frac{2Nh\beta\ LH\ D}{\dot{m}_a(C_{pa}+WC_{pv})}})$$
$$T_2 = T_1 + (T_s - T_1)(1 - e^{-\frac{2Nh\beta\ LH\ D}{\dot{m}_a(C_{pa}+WC_{pv})}}) \quad (33)$$

Equation (33) gives the temperature at the outlet of the packing.

In the present experimental setup, four packings are at four different positions and continuously reciprocate inside the duct. The specific humidity and outlet temperature after stage 1 are given by Equations (21) and (33). The first stage outlet values become the input conditions for stage 2 and this process continues. As a result of this, T_2 and T_3 are the intermittent temperatures and W_2, W_3 are the intermittent specific humidity values. Duct outlet air exits with the temperature T_4 and specific humidity W_4. Fig. 4 shows the psychrometric chart representing the temperature and humidity at various points calculated from the above method for the air entry velocity 5.6 m/s, RH 75% and for the cam speed of 10 rpm.

1, 2, 3 and 4 with dark black: Exit air conditions at the entry, exit of 1st, 2nd ,3rd and 4th packing respectively. Light black lines: Constant RH lines, Green lines: Constant enthalpy lines, Red lines: constant specific volume lines, Blue lines: DBT values.

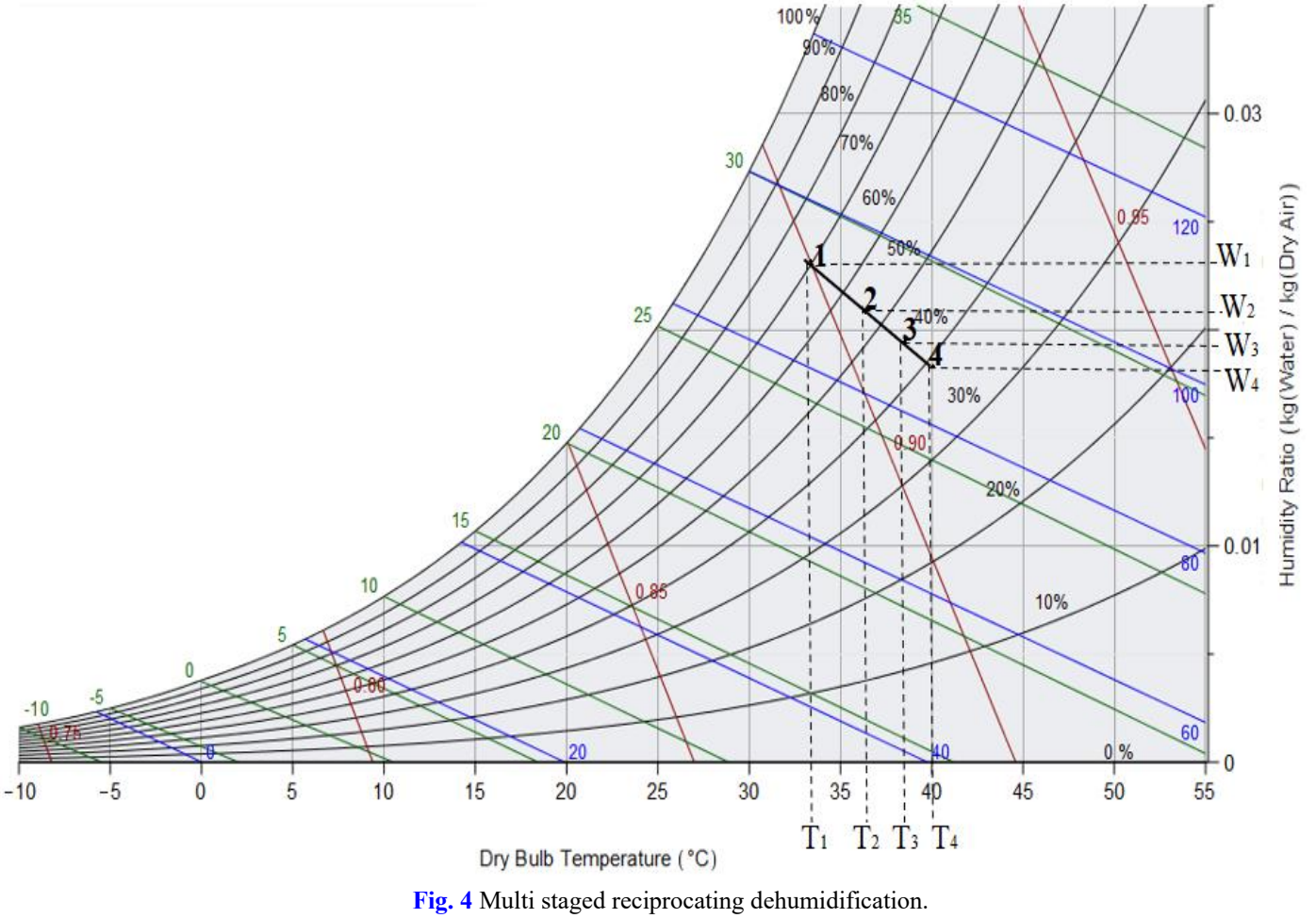

Fig. 4 Multi staged reciprocating dehumidification.

The MRR (moisture removal rate) is given by Equation (34), which is determined by the product of the difference in specific humidities at the inlet &outlet and air mass flow rate.[26]

$$MRR = (W_1 - W_4)\,\dot{m}_a \quad (34)$$

Moisture or dehumidification effectiveness is the ratio of specific humidity differences between inlet and outlet to the inlet equilibrium conditions. It is given by Equation (35).[31]

$$\varepsilon = \frac{W_1 - W_4}{W_1 - W_{eq}} \quad (35)$$

Mass transfer coefficient is the ratio of moisture removal rate to the product of surface area and difference in specific humidity between equilibrium and average conditions. Equation (35) gives the mass transfer coefficient. [26]

$$K = \frac{MRR}{A\,(\omega_{av} - \omega_{av,eq})} \quad (36)$$

3. Experimental test rig and working

3.1 Construction and working

Construction: Fig. 5 shows the schematic sketch of the dehumidification test rig. It mainly consists of absorber, regeneration unit, cooling system and vapor compression unit (VCR), which supply heat energy and provide cooling to the dehumidifier. It is an ordinary refrigeration system consisting of an evaporator, compressor and a condenser unit integrated with the dehumidification system. Evaporator coils cool the desiccant placed in the absorber tank and hence keeps the absorber desiccant temperature at a lower value and maintains it. Heat energy released by the condenser unit is utilized to heat the desiccant during regeneration. The absorber unit consists of four Celdek packing which are positioned at four different positions. The reciprocating motion is induced by the cam follower mechanism powered by 0.3 HP motor. By changing the diameter of the sprocket of the camshaft, the speed of the camshaft is varied. A hard thermocol duct, desiccant collector tank, reciprocating packing system forms the absorber unit. Regeneration unit mainly consists of a preheater and heater tank which regains the concentration of the desiccant. Radiator unit dissipates the heat and reduces the temperature of the desiccant. The desiccant used in the test rig is calcium chloride and the packing used is Celdek 7090. 20%, 30%, and 40% concentrations of $CaCl_2$ desiccant are prepared by mixing powdered $CaCl_2$ salt in water. Concentration is calculated using the weight ratio method where it is defined as the ratio of the weight of the solute to the weight of the solvent.[33] Hence prepared $CaCl_2$ solutions have been used for the experiments.

Working: Air is blown inside the duct by a 0.5 HP blower. It interacts with four reciprocating packings dipped in the desiccant. Air velocity at the inlet is controlled by using a regulator set at 3.2, 4.4, 5.6, 6.9 and 8.2 m/s. This interaction leads to the condensation of moisture from the air due to the vapor pressure difference between air and desiccant. Latent heat gets converted into sensible heat which increases the temperature of the air leaving the duct. Low concentration desiccant in the collector tank is circulated into the regeneration unit where it gets heated by the waste condenser heat from the VCR in a preheater. Then it is passed into a heater unit where the electric coil heats it to boiling temperature. Hot desiccant enters the separator which has baffles in it. Moisture and desiccant separates as the desiccant flows in the separator. When the concentration of the desiccant is increased, its vapor pressure will be reduced. The desiccant solution regains 100% concentration when it passes through the contact device where it comes in contact with the reciprocating packing. This also diminishes the temperature and restores the original concentration. This is due to the mass transfer between the hot desiccant and incoming fresh air inside the contact device through tiny openings. Vapor pressure difference leads to the moisture exchange and also cools the desiccant. Radiator cools the hot desiccant which is a second stage cooling and supplies it to the absorber where the temperature is regulated using the evaporator of the VCR system.

3.2. Experimental conditions

Dehumidification experiments are conducted by varying the input conditions. Camshaft or the motor shaft is operated at four different speeds 6, 10, 16 and 21 rpm and the air is blown at five different velocities 3.1, 4.4, 5.6, 6.9 and 8.2 m/s. Calcium chloride desiccant concentration is maintained at 20, 30 and 40% which flows with a constant flow rate of 30 LPM. (Liters per minute). Air and desiccant interact in the cross-flow direction. The value of dry bulb temperature, specific humidity, wet bulb temperature, air velocity and desiccant concentrations at the inlet and the outlet are recorded. Performance parameters such as moisture removal rate, mass transfer coefficient and dehumidification efficiency are determined using the expressions 34-36.

4. Specifications of measuring instruments and error analysis

4.1 Instrumentation

Digital thermometers are used to measure dry and wet bulb temperatures at the inlet and exit section having a range of -20 to 80 °C, resolution of 0.1°C and accuracy of ± 0.1 °C. A hygrometer is used to measure relative humidity has a range of 0%-99%, resolution 0.1% and accuracy ± 2.0%. An anemometer measures the air velocity with a range of 0.3 to 30 m/s, resolution 0.1 m/s and accuracy ± 5%. Tachometer measures the camshaft speed, which ranges 10 to 99999 rpm and resolution 0.1 rpm and accuracy ± 0.04%. A refractometer measures the desiccant concentration which reads the salinity content from 1-100% and has a resolution of 1%. The flow meter is used to measure the volume flow rate of the desiccant has a flow range of 10 to 120 Liters per minute (LPM) and has an accuracy ± 1%. Clamp meter measures instant voltage and current operates at a temperature of 0 to 40°C and RH less than 80%. Energy meter used to measure total power consumed has voltage of 220 V, frequency 50 Hz and current range 5 to 80 A.

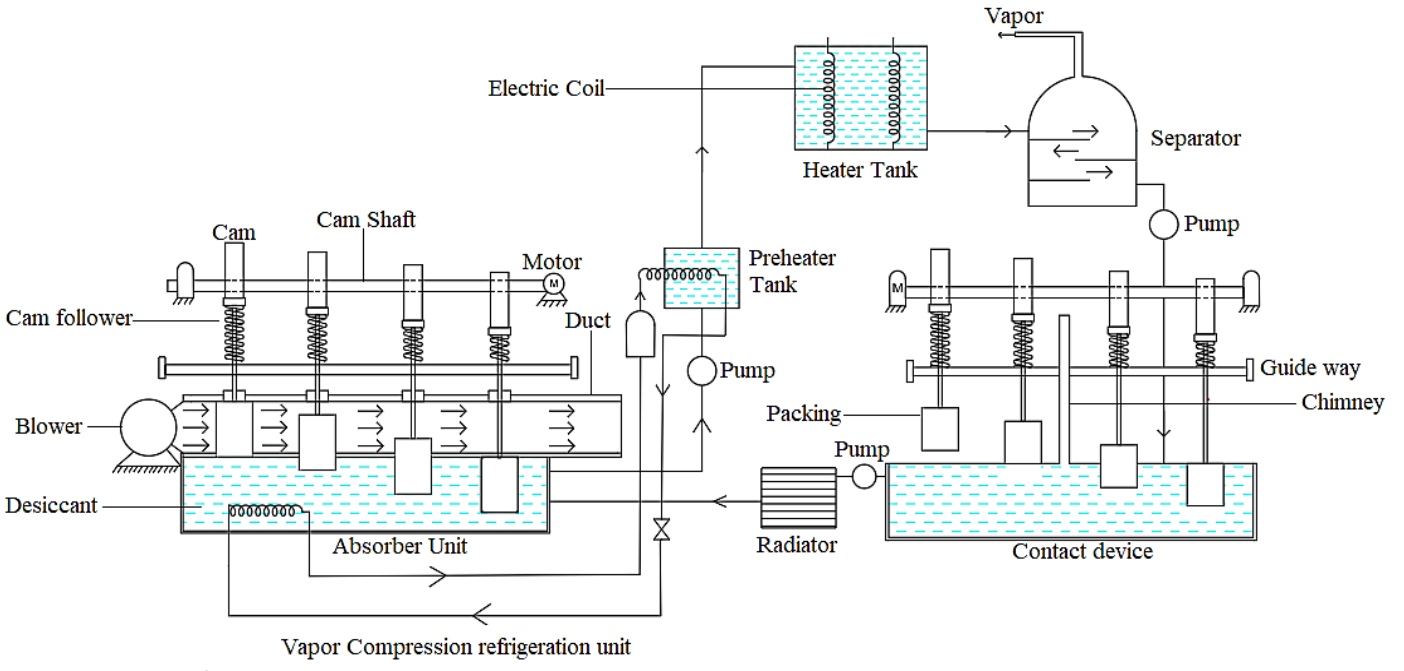

Fig. 5 Schematic sketch of multistage reciprocating dehumidification test rig with regeneration.

4.2 Error analysis

It mainly describes the deviation of the results due to the error present in the input experimental parameters.

Let X_1, X_2, ……., Xn be the independent variable and G be the function, Y_1, Y_2……Y_n be the uncertainty intervals and the uncertainty Y_G is given by Equation (37),

$$Y_G = \left[\left(\frac{\delta G}{\delta X_1} Y_1\right)^2 + \left(\frac{\delta G}{\delta X_2} Y_2\right)^2 + \left(\frac{\delta G}{\delta X_3} Y_3\right)^2 + \cdots\cdots\cdots + \left(\frac{\delta G}{\delta X_4} Y_n\right)^2\right]^{0.5} \quad (37)$$

Uncertainty in MRR is given,

$$\frac{\partial(\dot{m_W})}{\dot{m_W}} = \sqrt{\left(\frac{\partial \dot{m_a}}{\dot{m_a}}\right)^2 + \left(\frac{\partial \Delta W}{\Delta W}\right)^2} \quad (38)$$

Uncertainty in K or mass transfer coefficient is given by Equation (39),

$$\frac{\partial(K)}{K} = \sqrt{\left(\frac{\partial(\mathrm{MRR})}{\mathrm{MRR}}\right)^2 + \left(\left(-\frac{\partial(\mathrm{A})}{\mathrm{A}}\right)^2 + \left(-\frac{\partial(\Delta\omega_3)}{\Delta\omega_3}\right)^2\right)} \quad (39)$$

Dehumidification efficiency,

$$\varepsilon = \frac{\omega_i - \omega_o}{\omega_i - \omega_{eq}} = \frac{\Delta\omega_1}{\Delta\omega_2}$$

Uncertainty in moisture efficiency is described in Equation (40),

$$\frac{\partial(\varepsilon)}{\varepsilon} = \sqrt{\left(\frac{\partial\Delta\omega_1}{\Delta\omega_1}\right)^2 + \left(-\frac{\partial\Delta\omega_2}{\Delta\omega_2}\right)^2} \quad (40)$$

Uncertainty of the power consumed by the unit is given by

$$\frac{\partial(P)}{P} = \sqrt{\left(\frac{\partial V}{V}\right)^2 + \left(\frac{\partial I}{I}\right)^2} \quad (41)$$

By knowing the uncertainty of the input parameters, the total error in the output parameters is determined. Percentage uncertainty of moisture removal rate, dehumidification effectiveness, power consumed, and average mass transfer are found to be 2.48%, 1.48%, 2.48% and 2.38%, respectively.

5. Results and discussion

5.1 Desiccant concentration variation

Experiments are conducted by varying the air flow rate from 3.1 to 8.2 m/s and camshaft speed from 10-21 rpm. Three different desiccant concentrations 20%, 30% and 40% have been considered by fixing one camshaft speed. Outlet concentration depends on the inlet desiccant concentration, air flow rate, and specific humidities at the inlet and outlet. Fig. 6 shows the variation of the desiccant concentration with the air velocity. It is seen that concentration reduces slightly from its initial value, as the air velocity is increased. This may be due to the increased condensation rate of moisture at higher velocities. As the air velocity increases, the desiccant's moisture absorption rate increases and hence desiccant will be more diluted. This trend is observed for all the concentrations of the desiccants used. From the Figs. 6(a), 6(b) and 6(c), Concentration drops by 5.5%, 5.53% and 5.5% from the initial value of 20, 30 and 40 percentage when the air velocity increases from 3.1 m/s to 8.2 m/s. When the concentration of the desiccant increases, vapor pressure decreases and attracts more moisture.[26] When the desiccant absorbs the moisture, the latent heat of condensation will be converted to sensible heat, increasing the air and desiccant temperature. Both these factors influence the vapor pressure and hence dehumidification capacity of the desiccant decreases. Theoretical and experimental results are compared, and it is found that there is a deviation of 1.1%, 0.78% and 0.8% for 20%, 30% and 40% $CaCl_2$ solution and hence the developed model for predicting the outlet desiccant concentration is acceptable as the errors are within limits as compared with the literature.[1]

5.2 Variation of Cam shaft speed

5.2.1 Exit temperature and moisture removal rate

Fig. 7 gives the graphical representation of the exit dry bulb

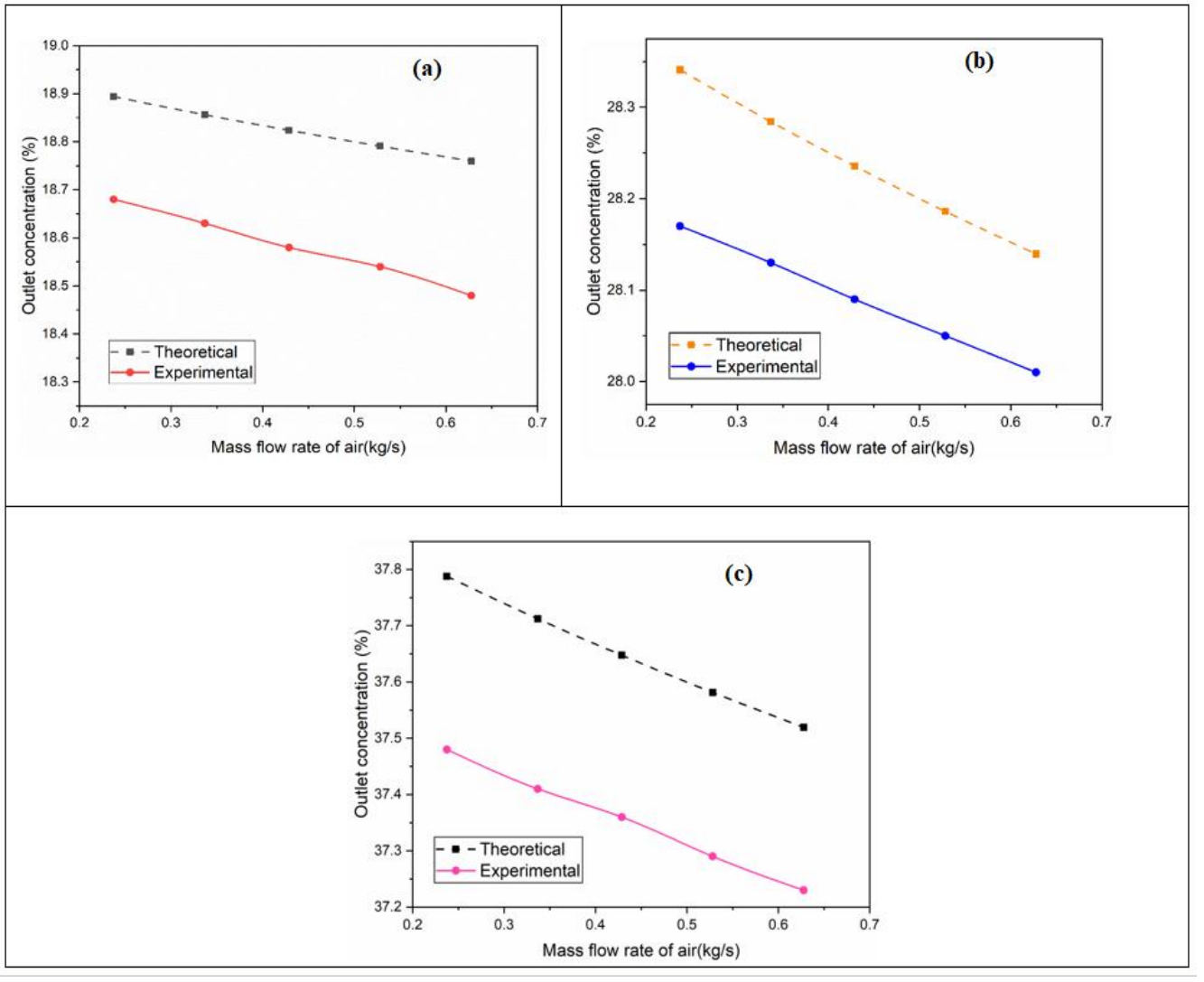

Fig. 6 Variation of outlet concentration with the mass flow rate of air for (a) 20% (b) 30% and (c) 40% of $CaCl_2$ desiccant Concentration.

temperature and the moisture removal rate with respect to the camshaft speed. Experiments are conducted for four different camshaft speeds 6, 10, 16 and 21 rpm. From the Figs. 7(a) & (b) is found that both exit temperature and MRR increase as the cam shaft speed is increased, attains a peak value at 10 rpm, and they drop significantly with further increase in cam rpm. When the cam rpm is changed, it varies the linear velocity of the packing that is reciprocating inside the duct. An increase in cam rpm increases the velocity of the reciprocating packing. This enhances the interaction between the packing and the air moving in the duct. Hence higher dehumidification takes place which reaches its maximum value at 10 rpm. Due to higher dehumidification, condensation rate will be increased and thus, more latent heat is converted into sensible heat.[2] This increases the outlet temperature as well as MRR. When the cam velocity surpasses 10 rpm, the contact time will be reduced as the linear velocity of the packing is very high. This again reduces MRR resulting in reduced exit temperature. For the tested range of the air velocities, predicted and experimental values for both MRR and exit temperature are very close, as seen from Fig. 8. For the optimum camshaft speed of 10 rpm and an airflow rate of 0.62 kg/s, outlet temperature and MRR theoretical and experimental values are deviated by 2.4% and 8.19%. The system gave a maximum MRR value of 5 g/s.

5.2.2 Mass transfer coefficient and moisture effectiveness

Mass transfer coefficient (MTC) mainly depends on the moisture removal rate. When the dehumidifier operates at a camshaft speed of 10 rpm, dehumidification is maximum and hence MTC also reaches the peak value. Further increase in the camshaft speed, due to the less contact time between air and the desiccant, MRR drops which also reduces the MTC. Fig. 8(a) shows when the camshaft speed increased from 10 to 21 rpm, there is a drop in the mass transfer coefficient by 31.42%, 36% and 33.33% for the air flow rate 0.62, 0.42 and 0.23 kg/s, respectively. Theoretical and experimental results showed that both have same trend and are very close to each other with a maximum deviation of 6.06%. With the increase in air velocity, there is a significant rise in the MRR due to

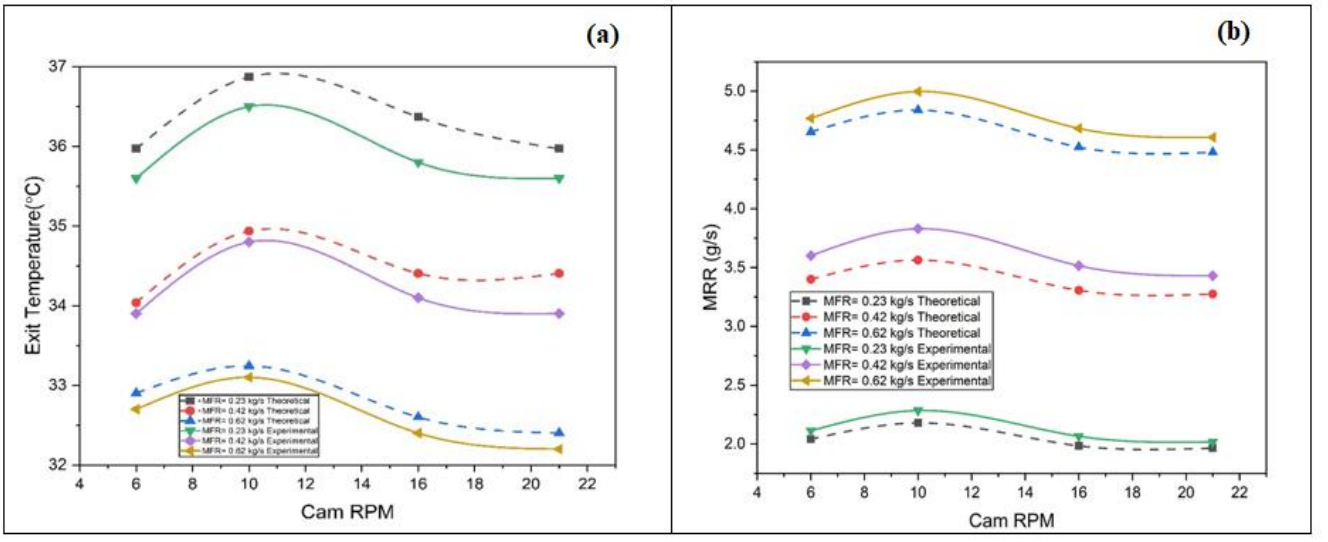

Fig. 7 Comparison of experimental and theoretical (a) exit air temperature and (b) moisture removal rate for various cam shaft speeds.

increased outlet-specific humidity and air mass flow rate. For a constant exposed area for dehumidification and concentration gradient, MTC is proportional to MRR. Moisture effectiveness is given by the ratio of the inlet to outlet specific humidity to the inlet to the equilibrium specific humidity. At the lower air velocity, the outlet specific humidity is low resulting in a huge specific humidity drop. This results in higher effectiveness. As the air velocity is increased, outlet specific humidity increases resulting in reduced moisture effectiveness and the obtained results are in line with the literature.[8] At 10 rpm, the condensation rate is higher therefore, the outlet specific humidity is low. This increases the specific humidity difference or moisture effectiveness. Desiccant interaction time with the humid air is higher at 10 rpm, which gives higher moisture effectiveness. Fig. 8(b) shows that the moisture effectiveness drops by 4.47%, 5.55% and 5.19% for air flow rate of 0.62 kg/s, 0.42 kg/s and 0.23 kg/s when the camshaft increased from 10 to 21 rpm. The predicted results from the developed model reveal that for the tested range of air velocities, moisture effectiveness is in good agreement with that of experimentally determined values. For lower air velocity and cam shaft speed of 10 rpm, theoretical results and experimental results are deviated by 5.47%, which are within the limits as observed from the literature.[1]

5.2.3 Outlet specific humidity

Fig. 9 gives the variation of the outlet specific humidity ratio with the camshaft speed, Outlet specific humidity is determined experimentally and evaluated theoretically. The outlet specific humidity drops when the camshaft speed is increased to 10 rpm. This drop is due to maximum condensation rate happening at this cam shaft speed. Good interaction between the desiccant and air can be attained at this speed, increasing the desiccant's moisture absorption rate. Because of the maximum moisture condensation occurring at this point, specific humidity decreases to the lowest value at

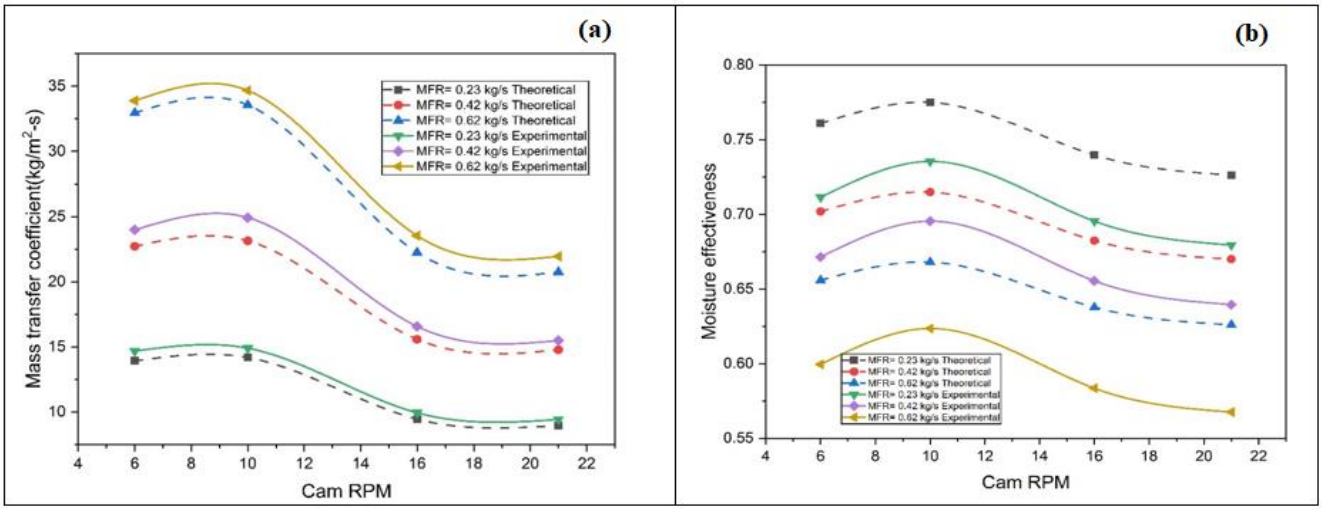

Fig. 8 Comparison of experimental and theoretical (a) mass transfer coefficient and (b) moisture effectiveness with the cam shaft speeds.

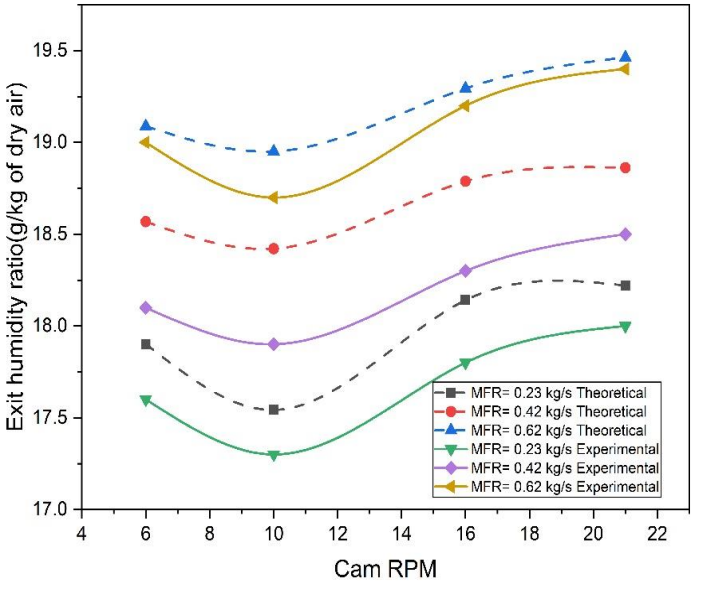

Fig. 9 Comparison of experimental and theoretical exit humidity ratio with the cam shaft speeds.

this point.[2] In other words, the difference in specific humidity or dehumidification will be maximum. When the theoretical and experimental results are compared, it is found that both are following the same trend and are close to each other, showing the acceptability of the developed theoretical model. A maximum deviation of 1.44% for air flow rate of 0.23 kg/s is noticed between the two which is acceptable. Results revealed that here is an increase in the outlet specific humidity by 2.85% when the camshaft speed rises from 10 to 21 rpm.

5.3 Variation of the packing thickness

To analyze the influence of pad thickness on the dehumidification performance, pad thickness is varied from 5 cm to 25 cm and the performance of the system is analyzed for various airflow rates keeping the camshaft speed at 10 rpm. The performance parameters have been determined and dehumidification performance is studied.

5.3.1 Outlet dry bulb temperature and specific humidity

Figs. 10(a) & (b) shows the variation of the exit temperature and the humidity ratio with the packing thickness. Mass flow rate is maintained at 0.23, 0.33, 0.42, 0.52 and 0.62 kg/s and the pad thickness are varied between 5 to 25cm. With the increase in the packing thickness, there is a rise in the dry bulb temperature and after the pad thickness of 20 cm there is a slight drop in the value. An increase in the exit temperature is associated with an increase in condensation rate or moisture absorbed by the desiccant. At lower thickness, the exposed area for the air to interact with the desiccant will be lower and hence lower dehumidification occurs. This increases as the thickness increases. But too high thickness increases the air passage time, distance through the pad, and weak interaction, thus reducing the outlet temperature. For the lower mass flow rate, the outlet dry bulb temperature is higher. Similarly, the outlet-specific humidity reduces until the pad thickness of 20 cm and the value remains constant. The dehumidification is effective till 20 cm thickness and the performance worsens further increase in the thickness, because it is difficult for air to pass through four thick packings and as a result of this, dehumidification performance deteriorates. DBT increases by 6.76% and specific humidity decreases by 23.63% when the pad thickness increases from 5 to 25 cm for air flow rate of 0.23 kg/s.

5.3.2 Moisture removal rate and moisture effectiveness

Figs. 11(a) & (b) gives the variation of the moisture removal rate and moisture effectiveness with the pad thickness. With the increase in pad thickness, MRR and moisture effectiveness rise by 33.33% and 60% for a mass flow rate of 0.23 kg/s. MRR and moisture effectiveness curves flattens or slightly falls when the packing thickness increases above 20 cm. When the packing thickness increases, moisture absorbed by the

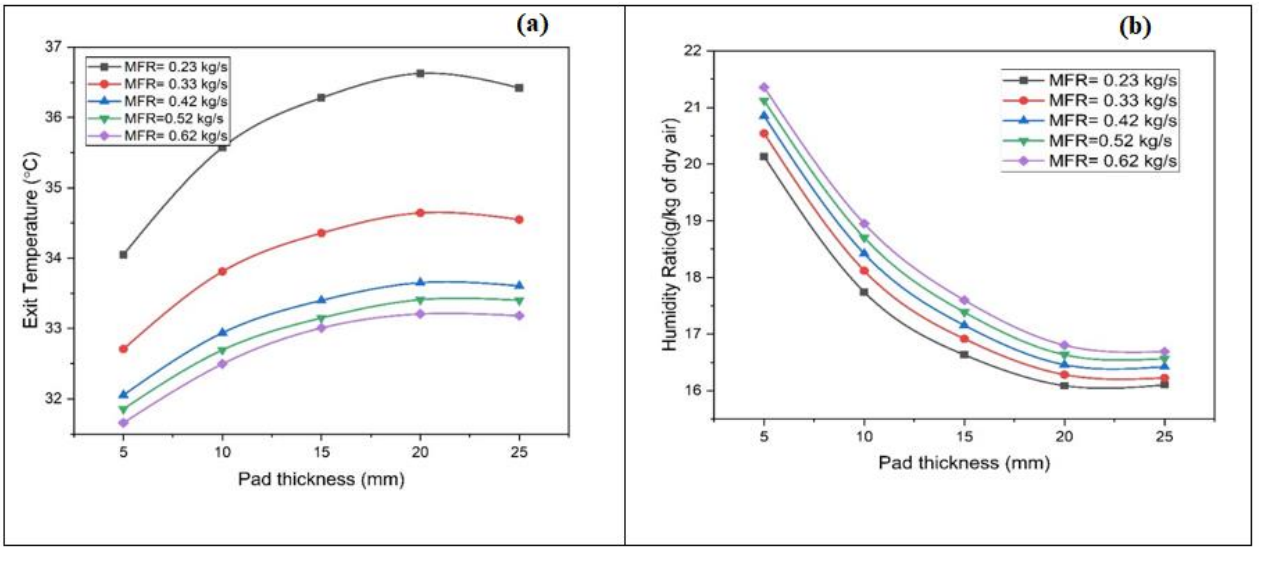

Fig. 10 Variation of (a) outlet DBT and (b) Specific humidity with the pad thickness and for different air mass flow rate.

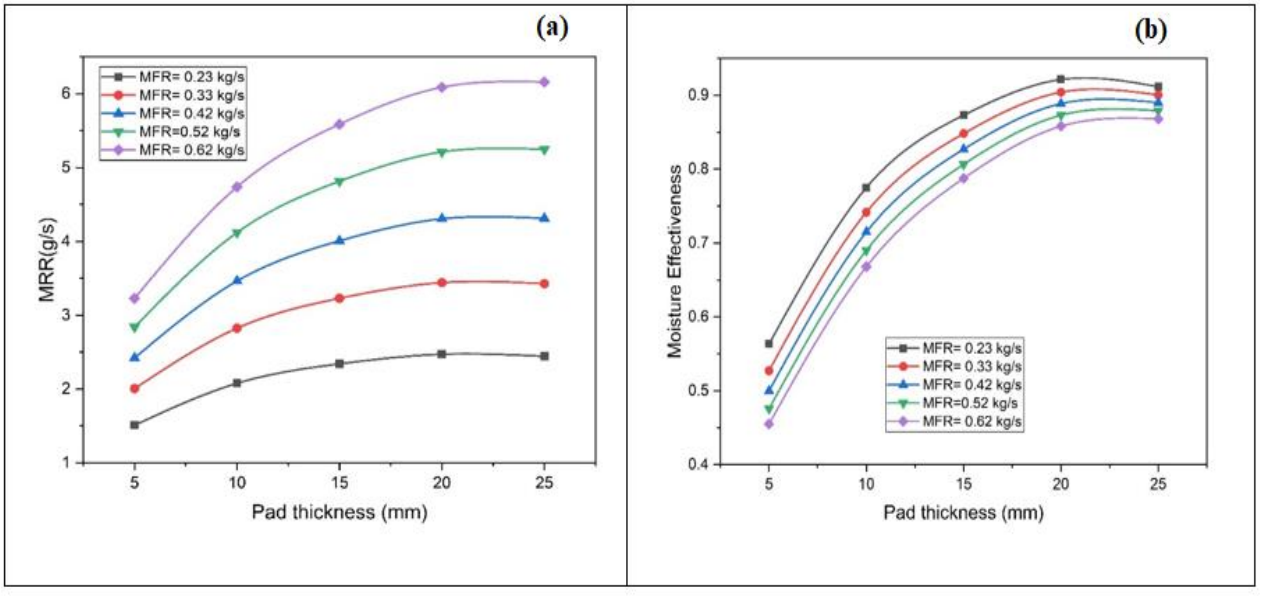

Fig. 11 Variation of (a) MRR and (b) moisture effectiveness with the pad thickness and for different air mass flow rate.

desiccant will increase which leads to rise in the dehumidification. Hence outlet specific humidity falls that leads to the rise in the MRR and moisture effectiveness. For 20 cm thickness when the mass flow rate increases from 0.23 to 0.62 kg/s, the MRR increases by 227.77%. Moisture effectiveness is found to be higher for lower air velocities or mass flow rates. As the mass flow rate is increased, moisture effectiveness drops. This may be due to the lower dehumidification performance at higher air velocities due to the reduced interaction between the desiccant and air. When the air mass flow rate is increased from 0.23 kg/s to 0.62 kg/s the moisture effectiveness decreases by 7.77% which means that moisture effectiveness is higher at lower air mass flow rate. The predicted results are in agreement with the reported literature values.[9]

5.3.3 Mass transfer coefficient (MTC)

Fig. 12 gives the mass transfer coefficient variation with the pad thickness. Since MTC is directly proportional to the MRR, MTC increases with the pad thickness. The airflow rate of 0.62 kg/s MTC increased by 88.88% when the pad thickness increased from 5 to 20 cm and the MTC value slightly dropped when the thickness is further increased. MTC is a direct indication of the moisture condensation that occurs when the desiccant comes in contact with air. The condensation rate increases when the pad thickness is increased.[26] With the rise in the airflow rate from 0.23 to 0.62 kg/s, there is a rise in the mass transfer coefficient by 207.14%.

From the results, it can be inferred that 20 cm thickness is the optimum thickness for the multistage reciprocating system as the dehumidification performance is maximum. Above 20 cm pad thickness, there is a drop in the dehumidification performance. In addition, higher thickness increases the pressure drop and hence there will be a considerable drop in the exit velocity. Also, the higher thickness increases the cost of pads.[20] Thus, from all these points for a multistage reciprocating dehumidification system using a 20 cm thick pad gives maximum performance.

Overall, when operated at 10 rpm, 30% desiccant concentration with pad thickness maintained at 20 cm, multistage dehumidification unit shows the optimum results. It is seen that the optimum values of MRR, moisture effectiveness and mass transfer coefficient were found to be 5.8 g/s, 0.80 and 42.5 kg/m^2-s respectively.

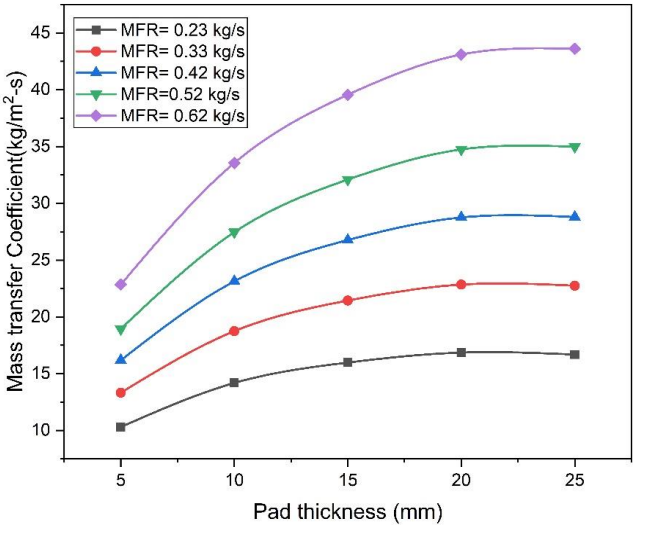

Fig. 12 Variation of Mass transfer coefficient with the pad thickness and for different air mass flow rate.

6. Validation of the results with the existing literature

The results obtained from the current study on the multistage reciprocating system are compared with the results obtained by the various researchers. Moisture removal rate and moisture effectiveness which are the important dehumidification parameters are compared with published literature and are shown in Figs. 13(a) & (b). The current

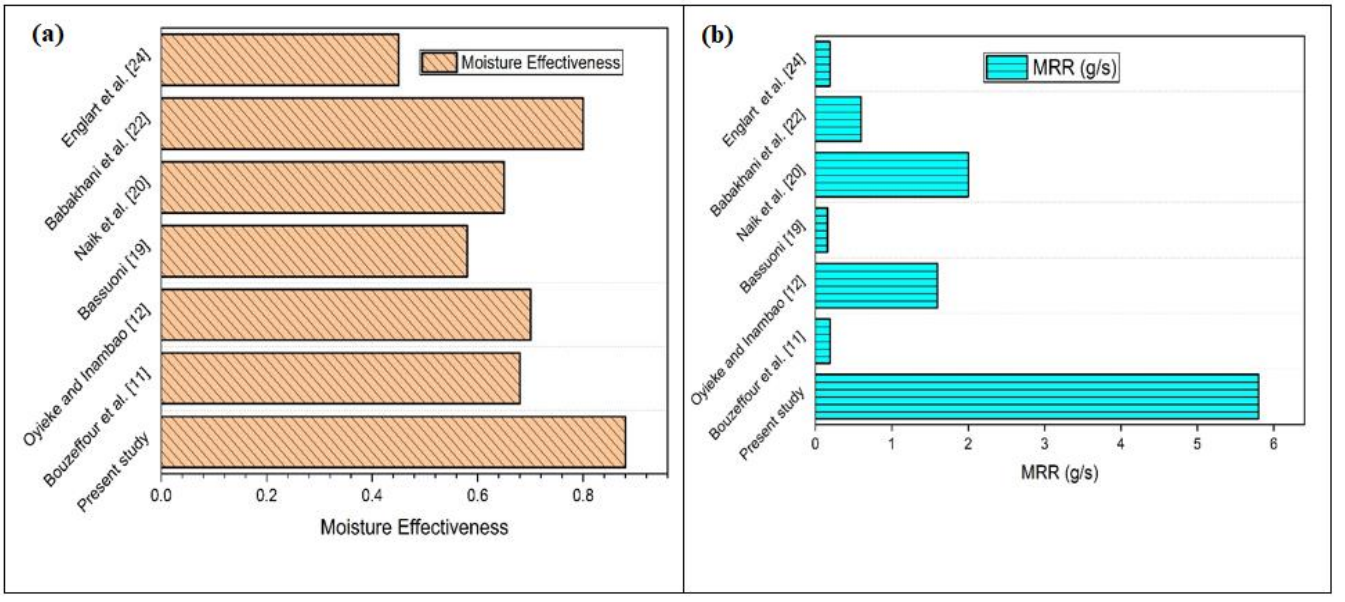

Fig. 13 Validation of the results with respect to (a) Moisture effectiveness (b) MRR.

system gave MRR and moisture effectiveness equal to 5.8 g/s and 0.88 which are higher than other systems. Multistage unit is also valuable as it provides high quality air, zero carry over, high energy efficiency and less time consumption for effective dehumidification or to attain thermal comfort. This justifies the use of the multistage reciprocating system over other existing single-stage stationary systems to have higher performance.

7. Conclusions

In the current study, an analytical model has been built to simulate and predict the performances of the multistage reciprocating dehumidifier system. The influence of camshaft speed, desiccant concentration and the packing thickness have been analyzed and the following conclusions are drawn.

Desiccant concentration dropped by 5.5%, 5.53% and 5.55% from their respective initial values for 20, 30 and 40 percent concentrations of $CaCl_2$ for the air mass flow rate equal to 0.23 g/s packing thickness 10 cm and camshaft speed of 10 rpm. This indicates the higher moisture absorption rate for higher concentrations of the desiccants. Experimental and theoretical results are very close to each other with an average deviation of 1.1%, 0.60% and 0.8% for 20%, 30% and 40% $CaCl_2$ solution for mass flow rate of 0.23 kg/s and camshaft speed of 10 rpm. 40% desiccant concentration corroded the system quickly and salts started accumulating which affected the flow. Cam speed of 10 rpm is considered as the optimum value for which maximum dehumidification performance has been noticed. Pad thickness of 20 cm is considered as the optimum pad thickness for the multistage reciprocating dehumidifier as the MRR and MTC are found to be maximum. Moisture effectiveness and mass transfer coefficient are 0.80 and 36 kg/m^2-s for camshaft speed of 10 rpm and packing thickness 20 cm. For 20 cm thickness, when the mass flow rate increases from 0.23 to 0.62 kg/s, there is an increase in the MRR by 227.77% and a drop in the moisture effectiveness by 7.77% which means that moisture effectiveness is higher at lower air flow rate.

The above study shows that multistage dynamic packing gave high dehumidification performance compared to the static single stage dehumidification system. Packing dipped inside the desiccant to minimize desiccant consumption, minimum carry over and ensued in minimum wastage of the desiccant. It also resulted in a lesser pressure drop. The present structure is an energy-efficient, sustainable technology-based system with reduced environmental pollution and provides high-quality indoor air. Theoretical prediction on the reciprocating multistage dehumidifier can be extended to different combinations of inputs, reducing the experimental effort, time, and financial investment.

Acknowledgments

Authors are thankful to the lab support provided by the School of Engineering & IT, Manipal Academy of Higher education, Dubai, UAE.

Conflict of interest

There are no conflicts to declare.

Supporting information

Not applicable.

Nomenclature

Variables/Parameters:	
C_P	Specific heat at constant pressure, kJ/kg°C
C_{Pa}	Specific heat at constant pressure of air, kJ/kg°C
C_{Pv}	Specific heat at constant pressure of Vapor, kJ/kg°C
C_{s1}, C_{s2}	Concentration of the desiccant at inlet and outlet, %

D	Depth of packing, m
h	Heat transfer coefficient, W/m^2°C
H	Height of packing, m
h_{a1}, h_{a2}	Specific enthalpy at the inlet and outlet, kJ/kg
K	Mass transfer coefficient, kg/m^2-s
L	Length of packing, m
LHV	Latent heat of vaporization, J/kg
$\dot{m}_a$	Mass flow rate of air, kg/s
MRR	Moisture removal rate, g/s
m_{s1}, m_{s2}	Mass flow rate of the desiccant at the inlet and outlet
N	Speed of rotation of the cam shaft, rpm
T_1	Inlet temperature, ℃
T_2	Outlet temperature, ℃
T_a	Air temperature, ℃
V	Air Velocities, m/s
Vp	Volume of the packing, m^3
$V_{Packing}$	Velocity of packing, m/s
W	Width of packing, m
W_1	Specific humidity at the inlet, g/kg
W_2	Specific humidity at the outlet, g/kg
We	Specific humidity of air at equilibrium, g/kg
β	Wettability, 1/m
ΔP	Change in the pressure, Pa
ΔT	Change in temperature, ℃
τ	Time period, Seconds
ρ	Density of air, kg/m3
Re	Reynold's Number
Pr	Prandtl Number
Nu	Nusselt Number
k	Thermal conductivity, W/m℃

Abbrevations

ANFIS	Adaptive Neuro Fuzzy Inference System
ANN	Artificial neural networking
CFD	Computational fluid dynamic approach
LDDS	Liquid desiccant dehumidification system
LPM	Liters per minute
LSSVM	least square support vector machine
MRR	Moisture removal rate
MTC	Mass transfer coefficient
VCR	Vapor compression refrigeration

Chemicals

$CaCl_2$	Calcium Chloride
HCO_2K	Potassium formate
Li Br	Lithium Bromide
Li Cl	Lithium chloride

References

[1] B. K. Naik and P. Muthukumar, *Build Environ.*, 2019, **149**, 330-348, doi: 10.1016/j.buildenv.2018.12.028.

[2] S. S. Sampath, S. Kumarand S. K. Reddy, *Int. J. Air-Cond. Refri.*, 2020, **28**, 1-16, doi: 10.1142/S2010132520300025.

[3] X. Ou, W. Cai, X. He, *Energy Build.*, 2019, **194**, 21-32, doi: 10.1016/j.enbuild.2019.04.019.

[4] N.A. Qasem, S. M. Zubair, *Desalination*, 2019, **461**, 37-54, doi: 10.1016/j.desal.2019.03.011.

[5] S. S. Salins, S. K. Reddy, S. Kumar, *Appl. Energy*, 2021, **293**, 116958, doi: 10.1016/j.apenergy.2021.116958.

[6] B. Kavasoğulları, E. Cihan, H. Demir, *Energy Procedia*, 2016, **91**, 785-791. doi: 10.1016/j.egypro.2016.06.244.

[7] M. T. Zegenhagen, C. Ricart, T. Meyer, R. Kühn, F. Ziegler, *Energy Procedia*, 2015, **70**, 544-551, doi: 10.1016/j.egypro.2015.02.159.

[8] A. Wu, C. Li, H. Zhang, *Int. J. Air-Cond. Refri.*, 2006, 1-9, http://citeseerx.ist.psu.edu/viewdoc/download?doi=10.1.1.839.5000&rep=rep1&type=pdf.

[9] S. Bouzenada, L. Frainkin, A. Léonard, *Procedia Comput. Sci.*, 2017, **109**, 817-824, doi: 10.1016/j.procs.2017.05.338.

[10] J. Lu, M. Wang, Y.Li, L. Yang, *Procedia Eng.*, 2017, **205**, 3630-3637, doi: 10.1016/j.proeng.2017.10.221.

[11] F. Bouzeffour, B. Khelidj, F. Yahi, D. Belkacemi, W. Taane, *Sci Technol Built Environ*, 2020, **27**, 211-225, doi: 10.1080/23744731.2020.1818504.

[12] A. Y. Oyieke, F. L. Inambao, *Int. J. Low Carbon Technol.*, 2019, **14**, 351-363, doi: 10.1093/ijlct/ctz022.

[13] A. Zendehboudi, A. Tatar, X. Li, *Renew. Energy*, 2017, **114**, 1023-1035. doi: 10.1016/j.renene.2017.07.078.

[14] D. Seenivasan, V. Selladurai, P. Senthil, *Adv. Mech. Eng.*, 2014, **6**, 506487, doi: 10.1155/2014/506487.

[15] E. Yohana, M. T. S. Utomo, Y. A. W. Arisandhy, E. Yulianto and M. Tauviqirrahman, *Int. J. Appl. Eng. Res.*, 2017, **12**, 1138-1141, http://www.ripublication.com/ijaer17/ijaerv12n7_03.pdf.

[16] S. Shen, W. Cai, H. Yon, Q. G. Wang, IEEE 11th Conference on Industrial Electronics and Applications (ICIEA), 2016, 1117-1121, doi: 10.1109/ICIEA.2016.7603750.

[17] W. Tao, L. Yimo, L. Lin, *Appl. Energy*, 2019, **240**, 486-498, doi: 10.1016/j.apenergy.2019.02.068.

[18] B. Sreelal, R. Hariharan, *Int. J. Emerg. Eng. Res. Technol.*, 2014, **2**, 142-152, http://www.ijeert.org/pdf/v2-i7/19.pdf.

[19] M. M. Bassuoni, *J. Adv. Res.*, 2014, **5**, 175-182, doi: 10.1016/j.jare.2013.02.002.

[20] B. L. Naik, M. Joshi, P. Muthukumar, M. Sultan, T. Miyazaki, R. R. Shamshiri, H. Ashraf, *Sustainability*, 2020, **12**, 10582, doi: 10.3390/su122410582.

[21] R. Chengqin, J. Yi, Z. Yianpin, *Sol. Energy*, 2006, **80**, 121-131, doi: 10.1016/j.solener.2005.01.007.

[22] D. Babakhani, M. Soleymani, *Int. Commun. Heat Mass Transf.*, 2009, **36**, 969-977, doi: 10.1016/j.icheatmasstransfer.2009.06.002.

[23] R. Kumar, A. K. Asati, *Int. J. Curr. Eng. Technol.*, 2014, **4**, 557-563, https://www.semanticscholar.org/paper/Simplified-Mathematical.

[24] S. Englart, K. Rajski, *Energies*, 2021, **14**, 3320, doi:

10.3390/en14113320.
[25] Q. Guo, X. Qi, P. Sun, P. Guo, *Adv. Mech. Eng.*, 2019, **11**, 1-18, doi: 10.1177/1687814019896147.
[26] S. S. Salins, S. K. Reddy, S. Kumar, *Build Environ.*, 2021, **205**, 108245, doi: 10.1016/j.buildenv.2021.108245.
[27] Z. Q. Xiong, Y. J. Dai, R. Z. Wang, *Appl. Energy*, 2009, **87**, 1495-1504, doi: 10.1016/j.apenergy.2009.08.048.
[28] Y. Chen, X. Zhang, Y. Yin, *Appl. Therm. Eng.*, 2015, **98**, 387-399, doi: 10.1016/j.applthermaleng.2015.12.066.
[29] S. W. L. Alan, M. R. Islam, K. J. Chua, *Energy Procedia*, 2017, **142**, 1009-1014, doi: 10.1016/j.egypro.2017.12.347.
[30] B.L. de Oliveira Campos, A. O. S. da Costa, E. F. da Costa Junior, *Solar Energy*, 2017, **157**, 321-327, doi: 10.1016/j.solener.2017.08.029.
[31] S. S. Salins, S. K. Reddy, S. Kumar, *Indoor Built Environ.*, 2021, doi: 10.1177/1420326X211008509.
[32] J. M. Wu, X. Huang, H. Zhang, *Appl. Therm. Eng.*, 2008, **29**, 980-984, doi: 10.1016/j.applthermaleng.2008.05.016.
[33] S. S. Salins, S. K. Reddy, S. Kumar, *Appl. Therm. Eng.*, 2021, **199**, 117546, doi: 10.1016/j.applthermaleng.2021.117546.

Author Information

Sampath Suranjan Salins *is working as Assistant professor (Senior scale) in Mechanical Engineering department in School of Engineering and IT at MAHE Dubai, UAE. His research interests include heat transfer in fins, refrigeration and air conditioning, desiccant based dehumidification and humidification.*

S.V. Kota Reddy *is working as Professor in Mechanical Engineering department at MAHE Dubai. He is also an Academic president of MAHE Dubai. His research interests include refrigeration and air conditioning, Humidification and dehumidification, solar air heaters and heat pumps.*

Shiva Kumar *is an Associate Professor (Senior Scale) in the Department of Mechanical and Manufacturing Engineering, at Manipal Institute of Technology, Manipal Academy of Higher Education, Manipal, India. His research interests include refrigeration and air conditioning, desiccant based dehumidification and humidification, Engine combustion, Alternative fuels, pollution.*